Japan-Bangladesh Joint Seminar on Advances in Bridge Engineering ISBN: 984-32-2520-6
Dhaka, Bangladesh. 10 August 2005

Analytical study on steel-concrete composite girders

Yoshiaki Okui *

Department of Civil & Environmental Engineering, Saitama University
255 Shimo Okubo, Saitama 338-8570, Japan

Abstract

Analytical study on steel-concrete composite girders is introduced in this contribution. The load-carrying capacity of the composite girders and designing shear connectors are mainly discussed. A finite element model that accounts for partial interaction between a concrete slab and a steel girder in composite beams is introduced. The model takes into account material non-linearity in concrete and steel, and shear-slip behavior in shear connectors as well as geometric non-linearity due to large displacements. It is shown that the model can simulate reasonably well the load-deflection and interfacial slip in composite beams. Parametric studies are carried out on a continuous composite girder bridge to investigate the effect of the shear-slip characteristics of shear connectors. Installing flexible shear connectors near an interior support is effective for reduction of extension strain in a concrete slab, but reduces the load-carrying capacity.

Keywords: composite girder, shear connector, partial interaction

1. Introduction

Recent design codes for continuous composite girders allow tensile cracking in a concrete slab near internal supports due to negative bending. Of course, the crack width must be limited within an allowable level to ensure durability of the concrete slab. An amount of reinforcement in the concrete slab is commonly increased to reduce the crack width. In structural analysis, concrete within the crack region is neglected, and only steel girder and reinforcement in the concrete slab are considered as an effective member. One of the issues in designing continuous composite girder is the functionality as well as a rational design method for shear connectors embedded in the cracked concrete slab. To clarify the function and to establish the design method, it is necessary to consider the effect of relative slip between the concrete slab and steel girder on mechanical behavior of composite girders.

* E-mail: okui@post.saitama-u.ac.jp

Other examples where the slip effects become important are flexible shear connectors and precast concrete slabs. The flexible shear connectors are installed at internal supports in order to reduce tensile stress and accordingly cracking in concrete slab. In composite girder bridges with precast concrete slabs, due to the limit of the spacing for in-situ concrete casting, it is not always possible to accommodate enough studs for full interaction.

In this contribution, a two-dimensional nonlinear finite element program for load-carrying capacity of steel-concrete composite beams with partial interaction has been developed. The program considers geometrical non-linearity due to large displacement and material non-linearity for steel and concrete. In order to take into account partial interaction effects, additional degree of freedoms representing the slip at an interface between the concrete deck and steel girder is introduced.

2. Fiber model for partial iteraction

In this section, the proposed finite element model is briefly introduced; see Peckley (1998) and Peckley & Okui (2000) for a detailed formulation. A composite beam is modeled as two fiber beam elements and an interfacial spring, which connects the beam elements. Figure 1 illustrates the modeling a composite beam by means of these beam elements and the interfacial spring as well as definitions of coordinates and symbols for displacements. The upper beam represents the concrete slab, and the lower beam the steel girder. The effect of local buckling in a steel section is neglected in this modeling.

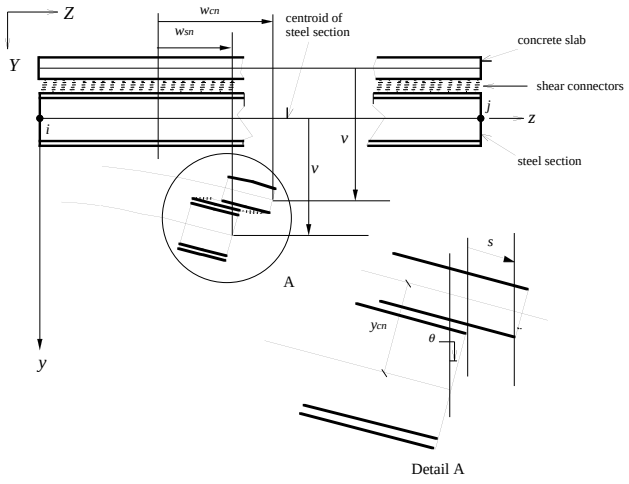

Fig. 1. Composite beam element and definition of coordinates and displacements.

Since the vertical displacements, rotations, and curvatures of these two beams are assumed to be identical, the displacements of both concrete and steel section can be expressed in terms of the axial and transverse displacements at the steel section centroid w_{sn}, v, and slip at the interface s. These displacements in an element are interpolated in terms of the shape function **H** and the nodal displacements:

$$w_{sn} = \mathbf{Hw}, \quad v = \mathbf{Hv}, \quad s = \mathbf{Hs} \tag{1}$$

where $\mathbf{w} = \{w_i, w_i', w_j, w_j'\}^T, \mathbf{v} = \{v_i, \theta_i, v_j, \theta_j\}^T, \mathbf{s} = \{s_i, s_i', s_j, s_j'\}^T$ and the prime stands for differentiation with respect to *z*; the Hermite function is employed as a shape function:

$$\mathbf{H} = [1 - 3(z/l)^2 + 2(z/l)^3, 1 - 2z^2/l + z^3/l^2, \\ 3(z/l)^2 - 2(z/l)^3, z^2/l + z^3/l^2] \tag{2}$$

where l = the length of an element.

Furthermore, fiber beam elements are employed for modeling the concrete slab and the steel girder to account for material nonlinearity. In each beam element, cross sections are considered to consist of thin steel or concrete layers subject to a different stress as shown in Fig. 2. The tangential stiffness of the beam element is evaluated in accordance with the tangential Young's modulus of the nonlinear stress-strain relation

The element stiffness matrix is evaluated by using the finite element method and the nonlinear strain-displacement equation including the finite displacement effect. An updated Lagrangian formulation is employed. The tangent stiffness matrix is obtained by integrating over the volume of an element including nonlinear stress-strain relations for steel and concrete, and slip-shear force relation at the interface. In the current formulation, effects of shear stress on the nonlinear stress-strain relations are neglected, and a simple fiber model with a uniaxial stress-strain relation is employed.

Finally, we have an incremental equilibrium equation for the nodal displacement and applied force:

$$[\mathbf{K} + \mathbf{K}_G]\Delta\mathbf{u} = \Delta\mathbf{P} \tag{3}$$

where $\Delta\mathbf{u} = \{\Delta\mathbf{w}, \Delta\mathbf{v}, \Delta\mathbf{s}\}^T$ and $\mathbf{K}$ = the tangential stiffness matrix due to material nonlinearity, $\mathbf{K}_G$ = the geometric stiffness matrix. Eq. (3) is solved for displacement increment $\Delta\mathbf{u}$ in an iterative manner until the unbalanced forces are within allowable tolerance.

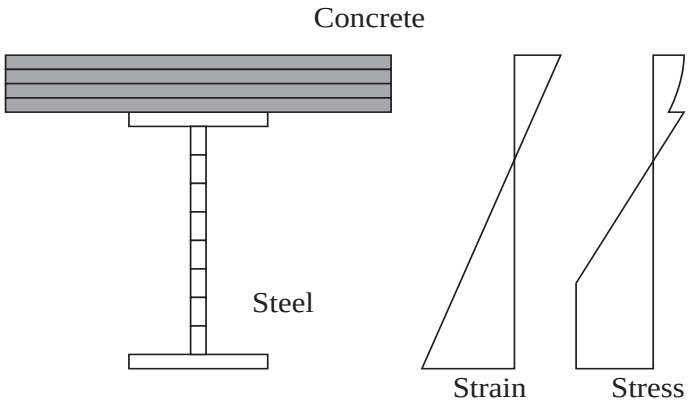

Fig. 2 Fiber beam element

3. Comparison with experimeant

To check the proposed model and program, comparison has been made with the test data reported by Nakajima & Ikegawa (1996). Figure 3(a) illustrates the experimental set up, and Fig. 3(b) shows the cross section of a specimen. This test specimen is designed to behave as a girder with partial interaction. The relative slip between the concrete slab and the steel girder on the shorter shear span is measured with clip-type gages. In addition, Nakajima & Ikegawa (1996) carried out push out tests of the same studs as the load-carrying test shown in Fig. 3. The reported slip-shear curve is used in the numerical analysis.

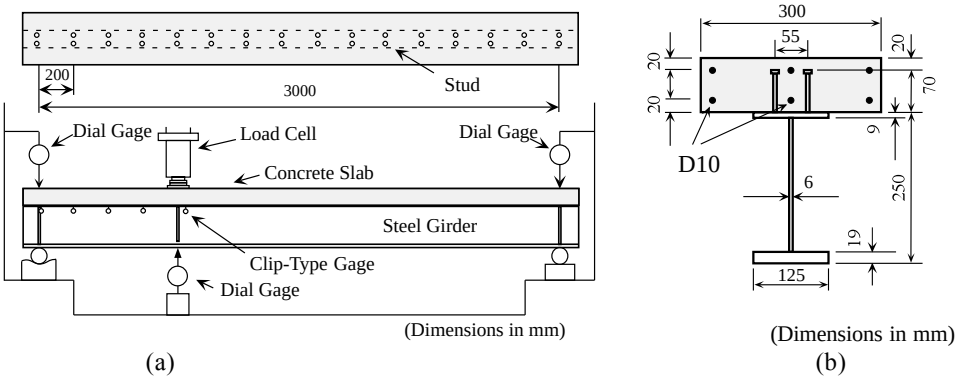

Fig. 3. (a)Test set-up; (b) Cross section of specimen from Nakajima et al. (1996).

Figure 4 shows the comparison of the load-deflection curves, and Fig. 5 is that of the load-slip curve. In both load-displacement and load-slip behavior, the numerical results are in good agreement with experiment ones.

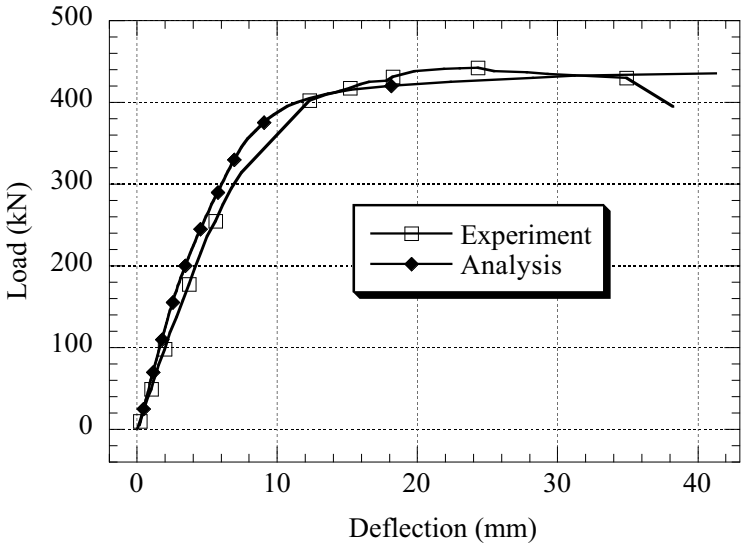

Fig. 4. Load-deflection curves.

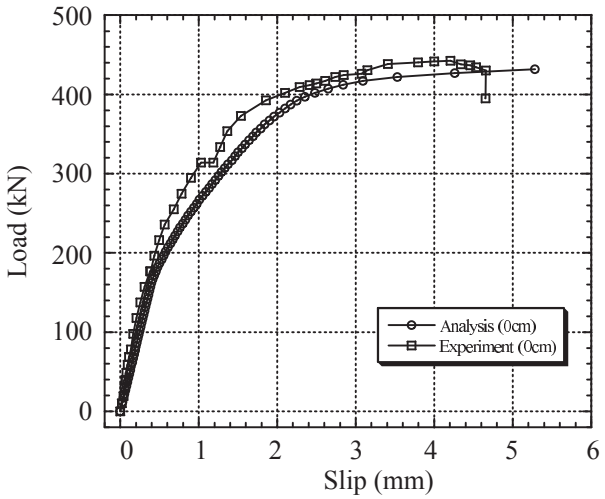

Fig. 5. Load-slip curves.

4. Parametric study for continuous bridge model

4.1 Structural model

In this section, we apply the proposed analytical method to the two-span continuous composite bridge shown in Fig. 6 (Japan Association of Steel Bridge Construction, 1995). The cross section of the model is shown in Fig. 7. The dimensions and yield stresses of the flange and web plates of the steel section are listed in Table 1. In designing this model bridge, cracking of the concrete slab near the internal support is assumed.

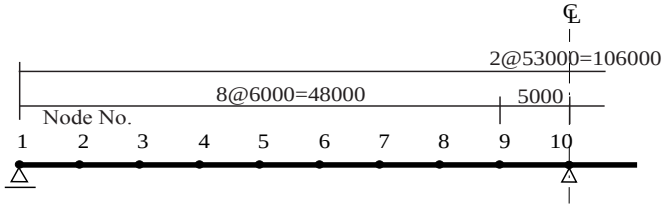

Fig. 6. Two-span continuous composite girder model (53+53 m) and dimensions of the steel girder (unit: mm).

For the stress-strain relation of steel, the simple elastic-perfectly-plastic model is used, while for concrete a parabolic-linear model (Fig. 8) is implemented in the program. The parabolic-linear model is given as

$$\sigma = \begin{cases} \sigma_{cm}\left[\dfrac{2\varepsilon}{\varepsilon_{cm}} - \left(\dfrac{\varepsilon}{\varepsilon_{cm}}\right)^2\right] & \text{for } (0 < \varepsilon < \varepsilon_{cm}) \\ \sigma_{cm}\left[1 - \dfrac{\varepsilon - \varepsilon_{cm}}{\varepsilon_{cu} - \varepsilon_{cm}}\right] & \text{for } (\varepsilon_{cm} < \varepsilon < \varepsilon_{cu}) \end{cases} \tag{4}$$

where the concrete strength σ_{cm}=35 MPa is used in the following analysis.

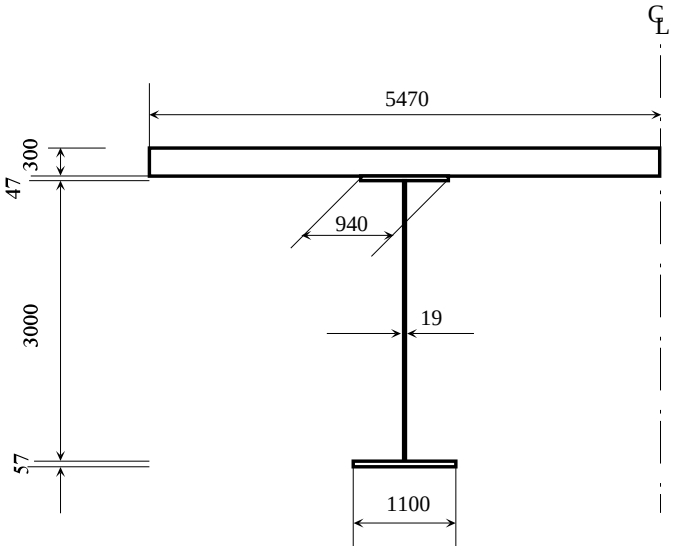

Fig. 7. Cross section near the interior support.

Table 1. Dimensions and yield stress of upper and lower flange plates

Position node-node	flanges			web	
	upper mm	lower mm	yield stress MPa	thickness mm	yield stress MPa
1-2	430x22	640x40	215	13	215
2-3	430x22	650x43	325	13	325
3-4	430x28	760x45	325	12	325
4-5	430x28	760x45	325	12	325
5-6	430x28	760x45	325	12	325
6-7	350x18	580x40	325	12	325
7-8	371x18	880x46	325	13	325
8-9	640x33	910x47	420	17	420
9-10	940x47	1100x57	420	19	420

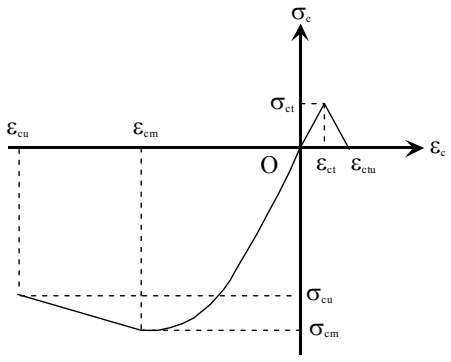

Fig. 8. Stress-Strain relation of concrete in compression.

Note that Eq. (4) is only valid in compression. The concrete in tension is neglected, but reinforcement steel in the RC slab is accounted as effective structural members. The tension stiffening effect in cracked RC members is also neglected in this treatment of concrete. The cross-sectional area ratio of reinforcement to the RC section is assigned to 1.5% in a negative bending region.

4.2 Shear connector

Two types of shear connectors are considered, namely conventional stud type connectors and a flexible shear connector proposed by Abe et al. (1989). The flexible shear connector is made of W-shapes (called H-shapes in Japan), whose web plate is covered with expanded polystyrene to enhance flexibility when it is embedded in a concrete slab. This flexible shear connector is specially designed to reduce tensile stress in the concrete slab near interior supports in continuous composite bridges. The flexible shear connectors have been installed in a railway bridge (Okuda et al., 1990).

The shear-slip relationships of these shear connectors are shown in Fig. 9, which is based on the push-out test results reported by Hosaka et al. (1998). Since it is seen that the tangential stiffness of the flexible shear connector after yielding is smaller than that of the shear studs, the flexible shear connector is more effective after the first yielding. Two cases for arrangement of shear connector are considered in the numerical analysis.

Figure 10 shows the distribution and types of shear connectors for both cases. In Case A, stud type connectors are used, and the pitch of shear studs is determined based on an elastic analysis following Japanese "Specification for Highway Bridges" (1992). On the other hand, in Case B, the flexible shear connectors are installed in the negative bending moment region near the interior support, and their pitch is determined according to that of slab anchors in non-composite bridges.

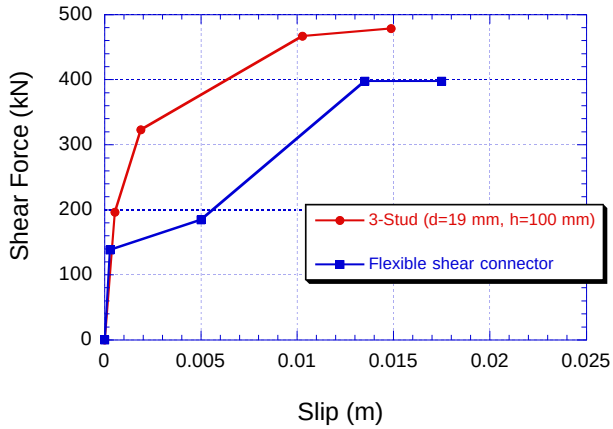

Fig. 9. Shear force-slip relationships of studs and flexible shear connector.

4.3 Load cases

In the following numerical analysis, the unshored construction is assumed. The dead load corresponding weight of steel girder and concrete (D_1=69.3 kN/m) is applied to the steel girder only, and then the superimposed dead load (D_2=13.7 kN/m) and the live load is applied to the composite section. In the following, the magnitude of the load is expressed in terms of the load factor α. The total load TL is given as

$$TL = \alpha(D+L) \tag{6}$$

where $D = D_1+D_2$ = Dead load, and L = Live load. Figure 11 shows considered loading cases in the numerical analysis. The intensity of the live and dead loads are 13.7 and 83.0 kN/m, respectively.

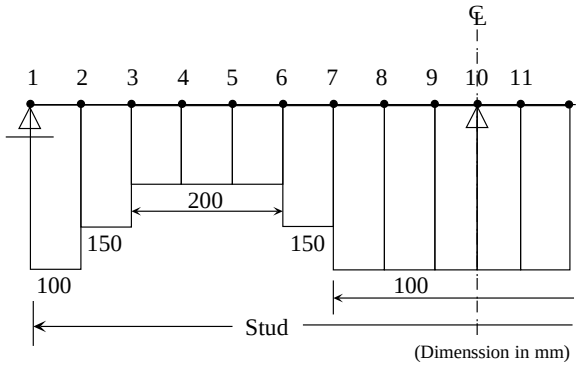

Fig. 10. Distribution of stud pitches and shear connector type; (a) Case A. (continue)

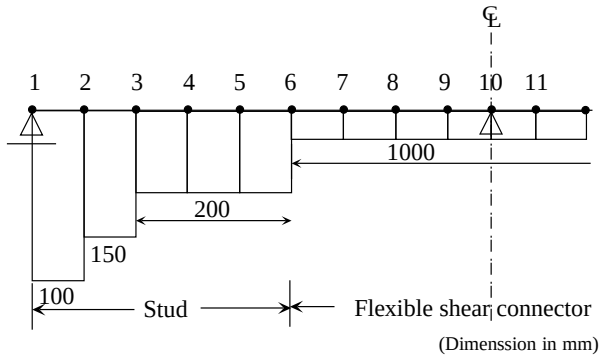

Fig. 10. Distribution of stud pitches and shear connector type; (b) Case B.

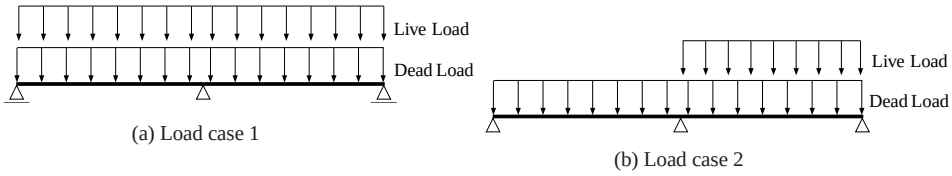

Fig. 11. Load cases; Dead and live load combination.

4.4 Effect of shear connector

Figures 12 shows the load-displacement curves for Load Case 1 and 2. The "Stud Case 1" stands for the original arrangement of studs defined in Fig. 10(a). The "Stud Case 2" and "Stud Case 3" , etc. mean 2 times and 3 times stud pitch of "Stud Case 1", respectively. In these figures, open circles and squares denote the ultimate points in the corresponding load-displacement curve. The circles express failure due to concrete crushing, while the squares due to failure of shear connector. By reducing shear

connector, the failure mode changes from concrete crushing to failure of shear connector.

The distributions of the relative slip along the bridge length at the maximum loading states are shown in Figs. 13 and 14 for Load Case 1 and 2, respectively. In the "Stud Case 1", the maximum slip for both cases are less than 0.005 mm, and the "Stud Case 1", in which studs arrangement is designed on the basis of the current Japanese Specification for Highway Bridges, is almost full interaction behavior. Even though the studs pitch is increased to twice of Case 1, the ultimate load-carrying capacity is governed by the concrete crushing and accordingly this situation is classified into full shear connection.

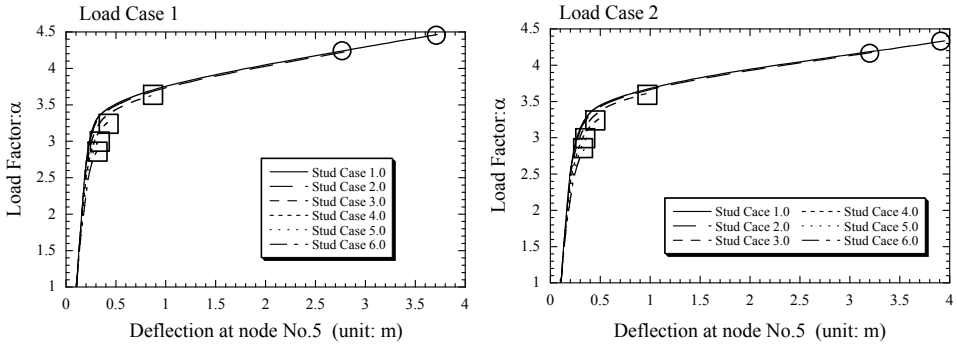

Fig. 12. Load-deflection curve for Load Case 1and 2.

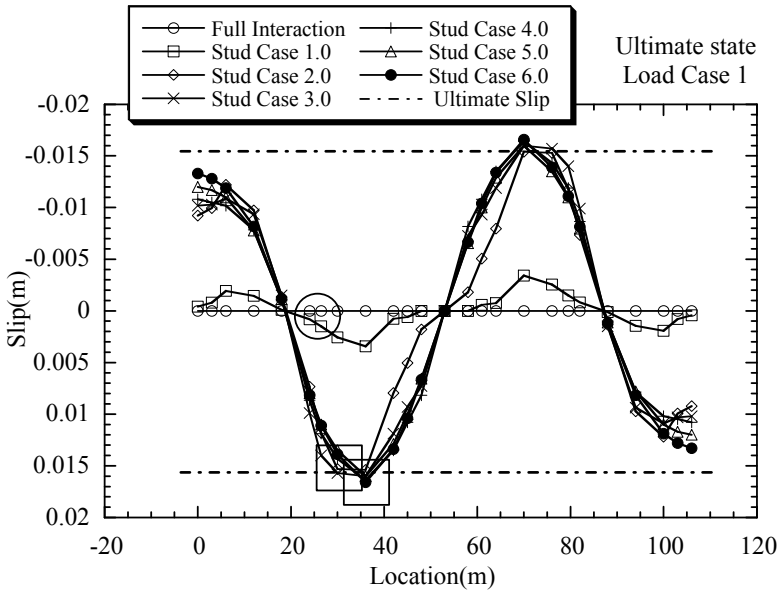

Fig. 13. Slip distribution along bridge at maximum loading for Load Case 1.

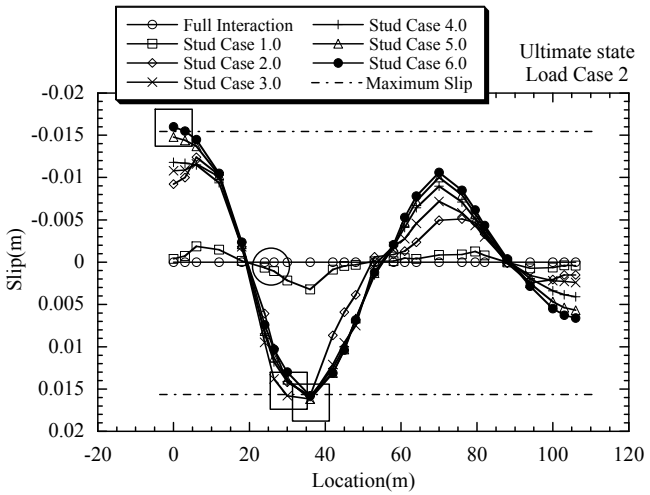

Fig. 14. Slip distribution along bridge at maximum loading for Load Case 2.

4.5 Flexible shear connector

Fig. 15 shows the bending moment diagram of both shear-connector cases at a service load of *D+L*. For these two cases, the difference of the maximum negative bending moments at the interior support is only 4%. Under service level loading, the reduction of negative bending moment at interior supports is not expected in spite of installing the flexible shear connector. However, it can be said that the increase in the maximum positive bending moment by installing the flexible shear connector is negligibly small as well.

To ensure durability of continuous composite bridges, it is important to control tensile cracks in a concrete slab owing to the negative bending moment. One objective for installing the flexible shear connector is to reduce crack width in a concrete slab. To check this aspect, the normal strain variations in the composite section at the interior support are plotted in Fig. 16, where the vertical axis stands for the vertical distance from the top of a concrete slab. In the shear-connector Case A, there is a slight strain jump at the interface between the concrete slab and steel girder. However, the behavior in Case A is practically full-interaction behavior. On the other hand, in Case B (flexible shear connector case) a considerable strain jump due to the slip occurs at the interface. Furthermore, the maximum strain in the concrete slab is reduced to 40 % of the strain in Case A. It is shown that the flexible shear connector is effective to reduce tensile strain, and accordingly tensile crack width in concrete slab.

5. Summary

In this contribution, a finite element model for load-carrying capacity of composite beams with partial interaction was introduced. The proposed model was applied to a two-span continuous composite bridge with two types of shear connectors. The numerical analysis shows that:

1. By installing flexible shear connectors, the load carrying capacity is decreased.
2. However, tensile strain at the internal support decreases, which is preferable from a crack-width control point of view.

3. The bending moment distribution at the service load level is not significantly affected by the flexible shear connector.

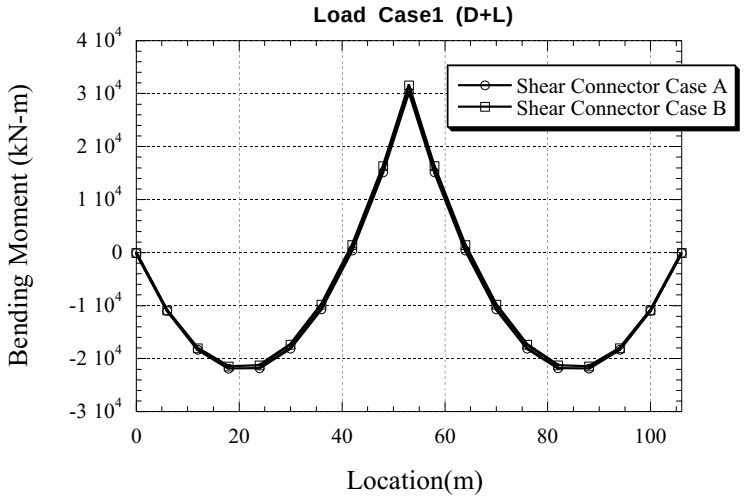

Fig. 15. Bending moment diagram for Load Case 1 at a service load level: Effect of shear connector cases on bending moment.

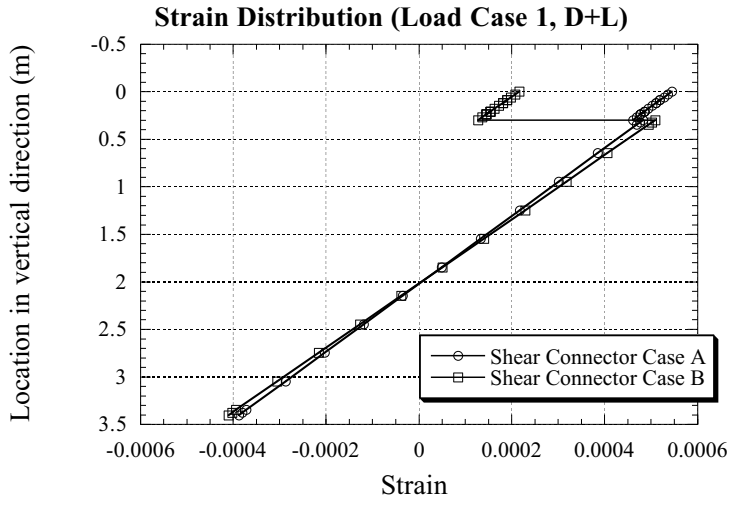

Fig. 16. Normal strain distribution in a plane at the interior support (profile view) for Load Case 1 at the service load.

References

Abe, H., Nakajima, A. & Horiuchi H., 1989. Effect of division of slab in composite girder and development of flexible connectors, *J. Structural Eng., JSCE*. 35A:1205-1214. (in Japanese)

CEN, 1996. EUROCODE4: Design of composite steel and concrete structures, Part 2: Bridge, 2nd draft.

Hosaka, T., Hiragi, H., Korda, Y., Tachibana, Y. & Watanabe, H. 1998. An experimental study on characteristics of shear connectors in composite continuous girder for railway bridges, *J. Structural Eng., JSCE*. 44A:1497-1504. (in Japanese)

Japan Road Association (JRA) 1992. Specification for high way bridges. Tokyo: Maruzen. (in Japanese)

Japan Association of Steel Bridge Construction (JASBC) 1995, Report on design of continuous composite bridges. (in Japanese)

Nakajima, A & Ikegawa, M. 1996. Elasto-plastic analysis of composite girder with inelastic behavior of shear connectors, *J. of Structural Mechanics & Earthquake Engineering, JSCE.* 43(591):97-106. (in Japanese)

Okuda, M., Satou, T., Yamaki, Y., Iseki, J. & Sasaki, H. 1990. Design and construction of Tokeidou3.4.20 viaduct in Hokusou line, *Bridge & Foundation.* 12: 13-22. (in Japanese)

Peckley Jr., D.C. 1998. Nonlinear analysis and ultimate strength of composite beams with partial interaction, Master thesis, Saitama University.

Peckley Jr., D.C & Okui, Y. 2000. A finite element model of steel-concrete composite beams and girders for near-collapse analysis, *Proc. Int. Conf. Concrete Art, Science and Technology, CAST2000, Manila*: Theme E: 1-17.

Okui Y., Seki K., Peckley D.C. 2001. Nonlinear analysis of load-carrying capacity for composite beams with partial interaction,., Proc. 1st Int. Structural Engineering and Construction Conf., pp.963-968.